



ON CHAOS IN GENERAL RELATIVITY

AUTHOR

MUHAMMAD HASHIR HASSAN KHAN

Department of Physics

Syed Babar Ali School of Science and Engineering

Lahore University of Management Sciences

LAHORE, MAY 2024

وَاللَّهُ الْمُسْتَعَانُ

And Allah is the One sought for help.

ON CHAOS IN GENERAL RELATIVITY

SUBMITTED IN PARTIAL FULFILMENT OF THE CONDITIONS FOR THE
AWARD OF THE DEGREE BS PHYSICS

AUTHOR

MUHAMMAD HASHIR HASSAN KHAN

Student No. 24100111

SUPERVISOR

SYED MOEEZ HASSAN, PHD


LAHORE, MAY 2024

Quaerendo invenietis.
By seeking, you will discover.

DECLARATION OF AUTHORSHIP

I declare on my honour that the work presented in this dissertation, entitled “On Chaos in General Relativity,” is original and was carried out by **Muhammad Hashir Hassan Khan** (24100111) under the supervision of Professor **Syed Moez Hassan, PhD** (syed_hassan@lums.edu.pk).

Lahore, May 2024

A handwritten signature in black ink, reading "Hashir Kh.", is written over a horizontal line. The signature is stylized with a large 'H' and a cursive 'Kh'.

Muhammad Hashir Hassan Khan

ACKNOWLEDGEMENTS

I am grateful.

To Mama and Baba for always being behind my back and for keeping up with me as I pushed another project to its absolute deadline.

To Dr. Syed Moez Hassan for being my supervisor and mentor by not only guiding me through this project but perhaps more importantly, for supporting me through unproductive days when working felt awful and nothing felt like it mattered any more.

To Dr. Rizwan Khalid for all the wonderful advice I received from him throughout my undergraduate journey and for turning up to the International Day of Mathematics celebrations.

To Dr. Imran Anwar, without whom, my society would not be what it is and through whom, I regained my love for mathematics popularization.

To my forever friends – Talha and Qais – for being there even when you're not.

To Qasim Javed for being the best friend there can be, looking after me and pushing me to be the best I could be (I am not sure I was) and for being the best caretaker of my society there could be.

To Abdullah Ahmed for being an inspiration from afar and for rekindling a love of problem-solving that I thought I had lost.

To Malaik Kabir for being the best SProj partner I could have wanted and for all the [redacted] jokes that I could laugh at for hours.

To my Physics fam – Rehan (for keeping up with your absent roommate), Daniel (for correcting my biryani-eating habits), Hamza (for introducing me to the dark side), Irtaza (for all the reassuring stickers that came my way), Abeera, Manahil, Hania – for all the days and nights spent in the department, enjoying and worrying together.

To my Physics juniors for showing up when it mattered.

And lastly, to my LSMS fam – Daniyal, Misbah, Ibrahim, Nabiha, Waleed, Ahmad, Mariam, Bilal, Qasim, Ayyan, Ayna, Abdullah Sohail, Abdullah, Zahra – I loved every single moment I spent with all of you.

ABSTRACT

Chaotic systems abound in nature. General relativity is the most non-linear theory there is. Surely, there must be chaos in general relativity. We attempt to look at this question by taking the homogenous, anisotropic Bianchi IX universe as a toy model. A short course on dynamical systems is prepared followed by a description of the Bianchi IX universe. Various indicators of chaos are applied to the Bianchi IX universe and their efficacy is judged. Finally, a short description of future possibilities is given.

CONTENTS

List of Figures	v
Acronyms	vi
Preface	vii
1 Dynamical Systems	1
1.1 Some Preliminaries	1
1.2 Two-Dimensional Linear Systems	4
1.3 Tackling Non-Linear Systems	11
2 The Bianchi IX Universe	19
2.1 The Metric and Some Calculations	19
2.2 The BKL Approximation	21
2.3 The Hamiltonian Formulation	22
3 Indicators of Chaos	23
3.1 What is Chaos?	23
3.2 Painlevé Test	24
3.3 Kolmogorov-Sinai (KS) Entropy for Discrete Maps	25
3.4 Liapunov Exponents	27
3.5 Fractals	28
4 A Glimpse Into the Future	30

LIST OF FIGURES

1.1.1 Phase portrait for $\dot{x} = x^2 - 1$. Note that the phase portrait consists only of the arrows and the horizontal line, not the blue graph.	3
1.1.2 Phase portrait for $\dot{x} = \sin x$	4
1.2.1 Phase portrait for a system with flow corresponding to clockwise rotation about the origin.	6
1.2.2 Phase portrait for a focus.	7
1.2.3 Phase portrait for a node.	8
1.2.4 Phase portrait for a line.	8
1.2.5 Phase portrait for a saddle.	9
1.2.6 Phase portrait for a Jordan node.	10
1.2.7 Phase portrait for a neutral line.	10
1.2.8 Phase portrait for a spiral.	11
1.3.1 Closed orbits in a conservative system.	13
1.3.2 Phase portrait for a nonlinear reversible system with a center at the origin.	15
1.3.3 Trapping region to apply the Poincaré-Bendixson Theorem.	17
2.1.1 A depiction of Euler angles.	19
3.1.1 Chaos abounds in nature.	24
3.5.1 The Sierpinski Triangle is a fractal.	28
3.5.2 Schematic of the box-counting dimension for an irregular area.	29

ACRONYMS

ADM	Arnowitt-Deser-Misner. (p. 22, 30)
BKL	Belinski-Khalatnikov-Lifshitz. (p. 21, 22, 25–27)
CMB	Cosmic Microwave Background. (p. 19)
DE	Differential Equation. (p. 1, 2, 4–6, 9–12, 24, 25)
EFes	Einstein Field Equations. (p. 19–21, 23, 30)
FLRW	Friedmann-Lemaître-Robertson-Walker. (p. 19)
GR	General Relativity. (p. 22–25, 27, 28, 30)
KS	Kolmogorov-Sinai. (p. iv, 25–27)
MSS	minisuperspace. (p. 22)
PP	Painlevé property. (p. 24, 25)

PREFACE

This thesis is written with a particular type of reader in mind – one who has taken a course on General Relativity and is familiar with the basic theory of differential equations. Some complex analysis and measure theory would be helpful but is not a requirement.

Chapter 1 is designed as a short course on dynamical systems. It takes the reader on a journey from one-dimensional systems to linear systems and finally to techniques used to tackle non-linear systems. Each section is equipped with solved examples to give the reader a taste of what problems to expect in this area. Apart from some linear algebra, the reader is not expected to have studied anything beyond a first-year undergraduate student to read through this chapter.

Chapter 2 is a description of the Bianchi IX universe. This is designed for readers who have taken General Relativity and are comfortable with calculating Christoffel symbols and Riemann curvature tensors on their own. A working knowledge of the ADM formalism would be helpful.

Chapter 3 works as a checklist for looking at chaos in General Relativity. Each section gives a flavour of what to expect and the reader is encouraged to read through other resources to gain a complete understanding.

Chapter 4 is a short look at future avenues of research in this area. No prior knowledge is required to read this chapter.

This thesis is not perfect, nor was it meant to be. At times, it may even seem chaotic. That the reader would have to embrace.

Happy reading!

DYNAMICAL SYSTEMS

What does an oscillating pendulum, the populations of rabbits and foxes in a national park and the Pakistan Stock Exchange have in common? They are all examples of *dynamical systems*. In this chapter, we shall build up the theory of dynamical systems from scratch, introducing various techniques and structures especially those used in the qualitative study of differential equations.

1.1 Some Preliminaries

Roughly speaking, a dynamical system is a system which evolves in time according to some fixed equation. For our purposes, the following precise definition suffices:

Definition 1.1.1 (Dynamical System). A dynamical system is a deterministic mathematical prescription for evolving the state of a system forward (or backward) in time.¹

In this work, we shall use the term dynamical system to refer both to the physical system as well as the mathematical set-up. Time may move forward in either discrete or continuous steps, dividing the area under study into the two streams of *discrete-time* and *continuous-time* dynamical systems. Our focus here, as in most physical applications, will be on continuous-time dynamical systems (although we will make use of discrete approximations later in this work). These systems are characterized by a Differential Equation (DE), together with initial conditions, of the following form:

$$\frac{d}{dt} \mathbf{x}(t) = \mathbf{F}[\mathbf{x}(t)]; \quad \mathbf{x}(0) = \mathbf{a}, \quad (1.1.1)$$

where $\mathbf{x}, \mathbf{a} \in \mathbb{R}^n$ and $\mathbf{F} : \mathbb{R}^n \rightarrow \mathbb{R}^n$. If \mathbf{F} depends explicitly on time, the system is called *non-autonomous*. Otherwise, the system is *autonomous*. Every non-autonomous DE can be converted to an autonomous one by introducing a new variable. Eq. (1.1.1) may seem very restrictive, considering that we are only looking at first-order DEs but, in fact, every n th order DE can be converted into a system of n first-order DEs. See Example 1.1.1 for an implementation.

¹ Adapted from (Ott, 2002)

Example 1.1.1 (Non-Autonomous Higher Order DE). Consider the equation for the damped, driven harmonic oscillator,

$$\ddot{x} + 2\beta\dot{x} + \omega_0^2 x = A \cos \omega t, \quad (1.1.2)$$

where the overdot represents a time derivative, β is a damping parameter and ω_0 is the natural frequency. To convert this into a dynamical system of the form (1.1.1), we begin by introducing the new variable $\mathbf{y} = (y_1, y_2)$ such that

$$\begin{aligned} y_1 &= x, \\ y_2 &= \dot{x}. \end{aligned} \quad (1.1.3)$$

Eq. (1.1.2) can now be written in the form of the following two equations:

$$\begin{aligned} \dot{y}_1 &= y_2, \\ \dot{y}_2 &= -2\beta y_2 - \omega_0^2 y_1 + A \cos \omega t. \end{aligned} \quad (1.1.4)$$

This remains a non-autonomous DE. To convert to an autonomous DE, we introduce the new variable $\mathbf{z} = (z_1, z_2, z_3)$ such that

$$\begin{aligned} z_1 &= y_1, \\ z_2 &= y_2, \\ z_3 &= \omega t. \end{aligned} \quad (1.1.5)$$

We can now rewrite eq. (1.1.2) as

$$\begin{aligned} \dot{z}_1 &= z_2, \\ \dot{z}_2 &= -2\beta z_2 - \omega_0^2 z_1 + A \cos z_3, \\ \dot{z}_3 &= \omega, \end{aligned} \quad (1.1.6)$$

which is manifestly in the form of eq. (1.1.6).

Our goal, in the theory of dynamical systems, is not to solve eq. (1.1.1) but to say something qualitatively about its solutions. To this end, we define a *phase space* composed of components of the variable \mathbf{x} . More precisely, we have the following definition:

Definition 1.1.2 (Phase Space). The phase space is the set of all possible states of a dynamical system, with each state representing one point in phase space.

In Example 1.1.1, the phase space is \mathbb{R}^3 since \mathbf{z} has 3 components with no restrictions on any of them. The path in phase space followed by the system as it evolves in time is called an *orbit* or a *trajectory*. The phase space together with a few sample trajectories drawn on it is called a *phase portrait*. To extract information from a dynamical system (which would be useful in drawing its phase portrait among other things), we would want to look at the form of $\mathbf{F}(\mathbf{x})$ in eq. (1.1.1). Generally, this could be any non-linear function. Therefore, we begin by finding out the *fixed points* of the system.

Definition 1.1.3 (Fixed Point). A fixed point \mathbf{x}^* of a dynamical system is a point where the system remains for all time once it enters it i.e. $\mathbf{x}(0) = \mathbf{x}^* \implies \mathbf{x}(t) = \mathbf{x}^* \quad \forall t \in \mathbb{R}$.

It is easy to see that a fixed point must satisfy $F(\mathbf{x}^*) = 0$. Example 1.1.2 illustrates these concepts.

Example 1.1.2 (Phase Portraits and Fixed Points). Consider the one-dimensional dynamical system,

$$\frac{dx}{dt} = x^2 - 1. \quad (1.1.7)$$

Here, $f(x) = x^2 - 1$. Solving for its zeroes, we get $x^* = \pm 1$. The phase portrait for the system is shown in Figure 1.1.1. The phase space is the x -axis and the function $F(x) = x^2 - 1$ is plotted for reference. Trajectories that move away from a fixed point are shown in red while those that move towards a fixed point are shown in purple. Note how the arrows seem to emerge from the fixed point at $x = 1$. This fixed point is therefore called a *source*. Further note how the arrows seem to go into the fixed point at $x = -1$. This fixed point is called a *sink*.

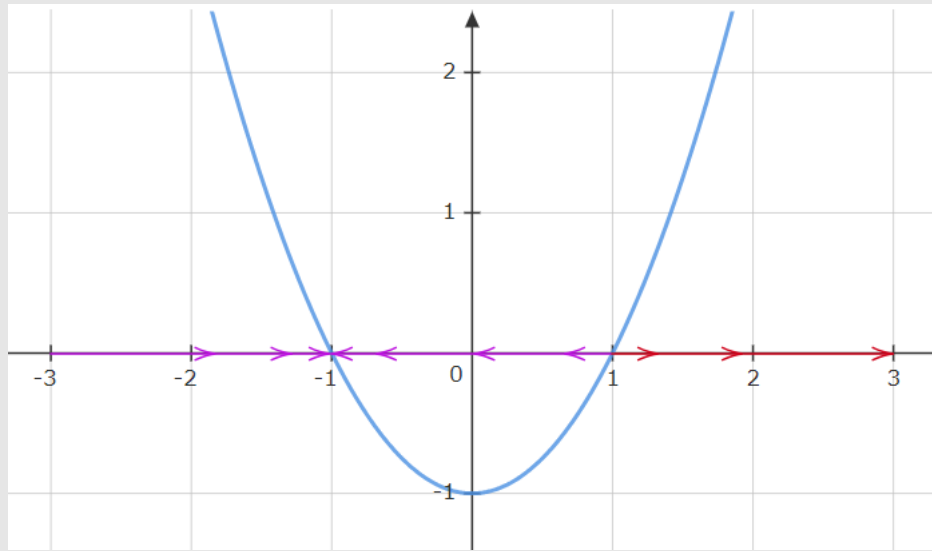


Figure 1.1.1: Phase portrait for $\dot{x} = x^2 - 1$. Note that the phase portrait consists only of the arrows and the horizontal line, not the blue graph.

Now, we shall study the stability of these fixed points in phase space. Intuitively, we want to understand what happens if we perturb the system slightly from its fixed point state. Consider a small perturbation $\mathbf{a}(t) = \mathbf{x}(t) - \mathbf{x}^*$ around the fixed point. Differentiating this w.r.t. t , we get

$$\dot{\mathbf{a}} = \dot{\mathbf{x}}. \quad (1.1.8)$$

Then, using a Taylor expansion for $F(\mathbf{x})$, we get

$$\begin{aligned} F(\mathbf{x}) &= F(\mathbf{x}^* + \mathbf{a}), \\ &= F(\mathbf{x}^*) + DF(\mathbf{x}^*)\mathbf{a} + \mathbf{R}, \\ &= DF(\mathbf{x}^*)\mathbf{a} + \mathbf{R}, \end{aligned}$$

where DF is the usual Jacobian and \mathbf{R} is the remainder term. Combining this with eqs. (1.1.1) and (1.1.8), we get a DE for the perturbation,

$$\dot{\mathbf{a}} = DF(\mathbf{x}^*)\mathbf{a}. \quad (1.1.9)$$

This equation not only describes how the perturbation grows over time but it is a dynamical system in its own right. When does this *linearization* about the fixed point give us accurate information about the physical system? This question shall be tackled in the next sections. For now, see Example 1.1.3 for an implementation of these concepts.

Example 1.1.3. Consider the one-dimensional dynamical system,

$$\dot{x} = \sin x. \quad (1.1.10)$$

The zeroes of the system are $x^* = n\pi$, where $n \in \mathbb{Z}$. Further, $F(x) = \sin x$ and $DF(x) = \cos x$. A linearization around a fixed point would be

$$\dot{a} = a \cos(n\pi) = \begin{cases} a & n \text{ is even,} \\ -a & n \text{ is odd.} \end{cases} \quad (1.1.11)$$

Therefore, around the fixed points, $F(x)$ can be approximated by a straight line. For even n , the perturbation $a(t)$ grows exponentially, suggesting that the fixed point is *attractive*. For odd n , the perturbation $a(t)$ decays exponentially, suggesting that the fixed point is *repulsive*. This can be confirmed using its phase portrait.

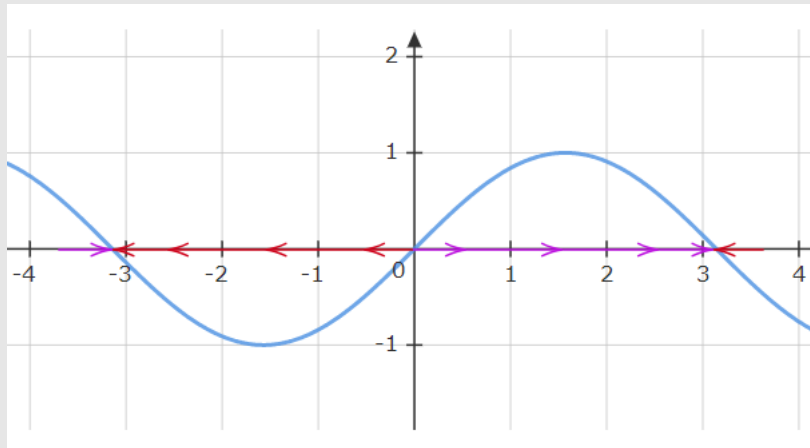


Figure 1.1.2: Phase portrait for $\dot{x} = \sin x$.

1.2 Two-Dimensional Linear Systems

One-dimensional systems are not of much further interest. We now begin looking at n -dimensional linear systems for which eq. (1.1.1) takes the form,

$$\dot{\mathbf{x}} = A\mathbf{x}; \quad \mathbf{x}(0) = \mathbf{a}, \quad (1.2.1)$$

where A is an $n \times n$ matrix. This system can be solved quite easily. Take $\mathbf{x} = \mathbf{a}e^{tA}$ as ansatz, where the exponential of the matrix is defined via its power series. Then, via familiar rules of differentiating the exponential of a matrix, it is easy to see that our ansatz satisfies eq. (1.2.1). This solution is so important that we give it a name – the *flow*.

Definition 1.2.1 (Flow). The flow of a DE is the 1-parameter family of maps defined by $g_t : \mathbb{R}^n \rightarrow \mathbb{R}^n$ such that

$$g_t(\mathbf{a}) = \mathbf{a}e^{tA}, \quad (1.2.2)$$

where $t \in \mathbb{R}$.

In simple terms, the flow describes the evolution of all initial states for a system. It takes a point \mathbf{a} (the initial state) and moves it around in phase space. Following this movement helps us visualize the *orbit* of \mathbf{a} . The following definition makes this idea precise.

Definition 1.2.2 (Orbit). The orbit (through \mathbf{a}) of a DE is the image set $\{g_t(\mathbf{a}); t \in \mathbb{R}\}$ corresponding to the solution curve $\mathbf{x}(t) = \mathbf{a}e^{tA}$. It is denoted by $\gamma(\mathbf{a})$.

Orbits can be broadly classified into two categories: *periodic orbits* corresponding to trajectories that return to the initial point after a finite time, and *non-periodic orbits* corresponding to trajectories that do not return in finite time. Note that *point orbits* corresponding to trajectories beginning at fixed points are a special case of periodic orbits. See Example 1.2.1 for an implementation of these concepts.

Example 1.2.1. Consider the two-dimensional DE,

$$\dot{\mathbf{x}} = \begin{pmatrix} 0 & 1 \\ -1 & 0 \end{pmatrix} \mathbf{x}. \quad (1.2.3)$$

Let A denote the matrix. To calculate its exponential, we find its first few powers.

$$A = \begin{pmatrix} 0 & 1 \\ -1 & 0 \end{pmatrix}, \quad A^2 = \begin{pmatrix} -1 & 0 \\ 0 & -1 \end{pmatrix}, \quad A^3 = \begin{pmatrix} 0 & -1 \\ 1 & 0 \end{pmatrix}, \quad A^4 = \begin{pmatrix} 1 & 0 \\ 0 & 1 \end{pmatrix}. \quad (1.2.4)$$

The flow can therefore be calculated as

$$\begin{aligned} e^{tA} &= I + tA + \frac{(tA)^2}{2!} + \dots, \\ &= \begin{pmatrix} 1 - \frac{t^2}{2!} + \frac{t^4}{4!} - \dots & t - \frac{t^3}{3!} + \frac{t^5}{5!} - \dots \\ -t + \frac{t^3}{3!} - \frac{t^5}{5!} + \dots & 1 - \frac{t^2}{2!} + \frac{t^4}{4!} - \dots \end{pmatrix}, \\ &= \begin{pmatrix} \cos t & \sin t \\ -\sin t & \cos t \end{pmatrix}. \end{aligned} \quad (1.2.5)$$

It can be clearly seen that the flow corresponds to clockwise rotation about the origin in two dimensions. Furthermore, due to the periodicity of the trigonometric functions, every orbit is a periodic orbit with period 2π apart from $\gamma(\mathbf{0}) = \{\mathbf{0}\}$ which is a point orbit. With a little thought, one can conclude that all orbits are circles. In fact, orbits

passing through \mathbf{a} have radius $|\mathbf{a}|$ i.e.

$$\gamma(\mathbf{a}) = \{x_1^2 + x_2^2 = |\mathbf{a}|^2; x_1, x_2 \in \mathbb{R}\}. \quad (1.2.6)$$

This can be seen in the phase portrait of the system as well. This time, the phase portrait is a phase plane and a few orbits have been drawn by connecting flow arrows.

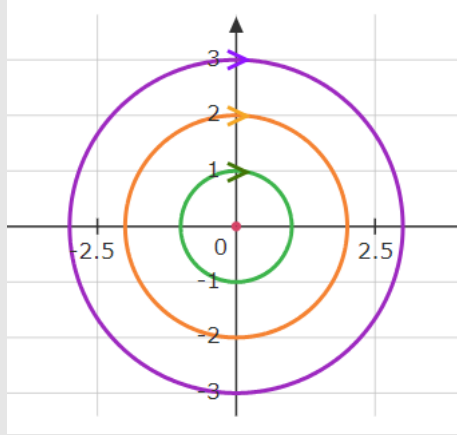


Figure 1.2.1: Phase portrait for a system with flow corresponding to clockwise rotation about the origin.

We would now want to classify the behaviour around a fixed point for all possible two-dimensional linear systems. Therefore, in what follows, we will try to solve eq. (1.2.1) for the two-dimensional case. To go from one linear system to another requires a linear transformation for both the time and space variables:

$$\begin{aligned} \tau &= kt, \\ \mathbf{y} &= P\mathbf{x}. \end{aligned} \quad (1.2.7)$$

Differentiating the second equation here w.r.t. τ gives

$$\begin{aligned} \dot{\mathbf{y}} &= P \frac{d\mathbf{x}}{d\tau}, \\ &= \frac{1}{k} P \frac{d\mathbf{x}}{dt}, \\ &= \frac{1}{k} P A \mathbf{x}, \\ &= \frac{1}{k} P A P^{-1} \mathbf{y}, \end{aligned} \quad (1.2.8)$$

where the overdot indicates a derivative w.r.t. τ and we used eqs. (1.2.1) and (1.2.7) in the third and fourth lines. Eqs. (1.2.8) and (1.2.1) are said to be *linearly equivalent*.

Definition 1.2.3 (Linear Equivalence). Two DEs with matrices A and B are called linearly equivalent if there exists $k \in \mathbb{R}$ and a matrix P such that $B = kPAP^{-1}$.

The matrix placement in the final answer $J = PAP^{-1}$ allows us to use the *Jordan canonical form* of A to describe all possible cases of two-dimensional linear systems.

Recall that for every two-dimensional matrix, we can find a non-singular matrix P such that $J = PAP^{-1}$ and J can have one of the following forms:

$$\begin{pmatrix} \lambda_1 & 0 \\ 0 & \lambda_2 \end{pmatrix}, \quad \begin{pmatrix} \lambda & 1 \\ 0 & \lambda \end{pmatrix}, \quad \begin{pmatrix} \alpha & \beta \\ -\beta & \alpha \end{pmatrix}, \quad (1.2.9)$$

We shall solve eq. (1.2.8) with $PAP^{-1} = J$ and $k = 1$ for all the aforementioned cases to find what are called *canonical linear flows*. In each of the following, y_1 and y_2 denote the components of \mathbf{y} , b_1 and b_2 denote the components of the initial state \mathbf{b} and $\mathbf{0}$ is a fixed point.

- **Case 1.** Using eq. (1.2.2) and recalling that the exponential of a diagonal matrix has the diagonal entries exponentiated, we get the following set of orbits:

$$\gamma(\mathbf{b}) = \left\{ \begin{pmatrix} e^{\lambda_1 t} b_1 \\ e^{\lambda_2 t} b_2 \end{pmatrix}; t \in \mathbb{R} \right\} \quad (1.2.10)$$

To visualize and plot them on a $y_1 y_2$ -plane, we solve the simultaneous equations,

$$\begin{aligned} y_1 &= e^{\lambda_1 t} b_1, \\ y_2 &= e^{\lambda_2 t} b_2, \end{aligned} \quad (1.2.11)$$

to get

$$\begin{aligned} \left(\frac{y_1}{b_1} \right)^{\frac{1}{\lambda_1}} &= \left(\frac{y_2}{b_2} \right)^{\frac{1}{\lambda_2}}, \quad \text{if } b_1, b_2 \neq 0; \\ y_1 &= 0, y_2 \text{ arbitrary}, \quad \text{if } b_1 = 0; \\ y_2 &= 0, y_1 \text{ arbitrary}, \quad \text{if } b_2 = 0. \end{aligned} \quad (1.2.12)$$

We now plot the phase plane for different values of λ_1 and λ_2 . We find the following results.

1. When $\lambda_1 = \lambda_2$, we have a *focus*. If both of them are positive (negative), the focus is called *repelling* (*attracting*). **Figure 1.2.2** shows the relevant phase portrait without arrows.

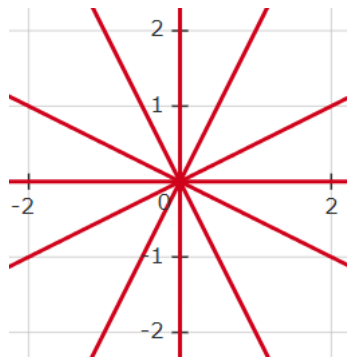


Figure 1.2.2: Phase portrait for a focus.

2. When λ_1 and λ_2 have non-zero values with the same sign and $\lambda_1 \neq \lambda_2$, we have a *node*. If both of them are positive (negative), the node is called *repelling* (*attracting*). When $|\lambda_1| < |\lambda_2|$, the orbits will move faster along the y_2 direction and vice versa. **Figure 1.2.3** shows the phase portrait for $|\lambda_1| > |\lambda_2|$.

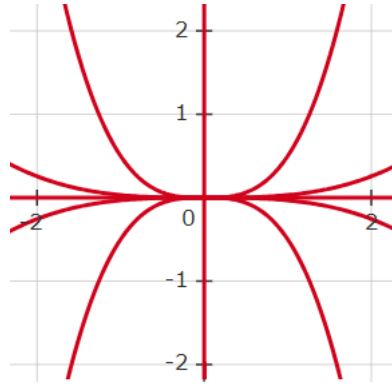


Figure 1.2.3: Phase portrait for a node.

3. When either λ_1 or $\lambda_2 = 0$ but not both, we have a *line*. If the non-zero value is positive (negative), the line is called *repelling* (*attracting*). If $\lambda_1 = 0$, the lines are parallel to the y_1 -axis and vice versa. **Figure 1.2.4** shows the phase portrait for $\lambda_1 = 0$.

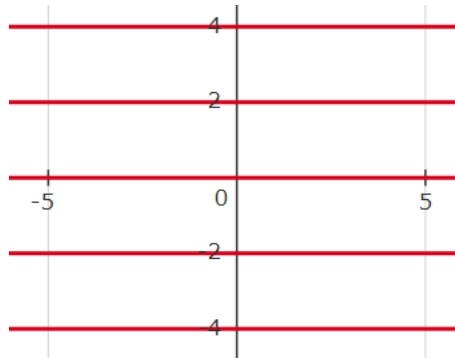


Figure 1.2.4: Phase portrait for a line.

4. When λ_1 and λ_2 have different signs, we have a *saddle*. If $\lambda_1 < 0 < \lambda_2$, we have attraction along the y_1 -axis and repulsion along the y_2 -axis and vice versa. **Figure 1.2.5** shows the phase portrait for $\lambda_1 < 0 < \lambda_2$.

- **Case 2.** Constructing a power series for J , we have

$$J = \begin{pmatrix} \lambda & 1 \\ 0 & \lambda \end{pmatrix}, \quad J^2 = \begin{pmatrix} \lambda^2 & 2\lambda \\ 0 & \lambda^2 \end{pmatrix}, \quad J^3 = \begin{pmatrix} \lambda^3 & 3\lambda^2 \\ 0 & \lambda^3 \end{pmatrix}, \quad J^4 = \begin{pmatrix} \lambda^4 & 4\lambda^3 \\ 0 & \lambda^4 \end{pmatrix}, \dots \quad (1.2.13)$$

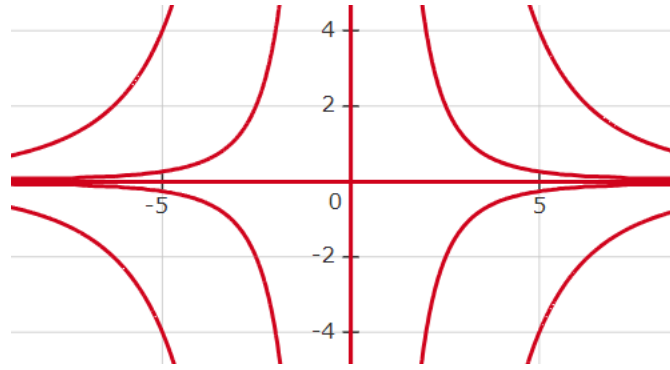


Figure 1.2.5: Phase portrait for a saddle.

Using this, we can write down the flow as

$$e^{tJ} = \begin{pmatrix} 1 + \lambda t + \frac{(\lambda t)^2}{2!} + \frac{(\lambda t)^3}{3!} + \dots & t + \lambda t^2 + \frac{\lambda t^3}{3!} + \frac{\lambda t^4}{4!} + \dots \\ 0 & 1 + \lambda t + \frac{(\lambda t)^2}{2!} + \frac{(\lambda t)^3}{3!} + \dots \end{pmatrix}, \quad (1.2.14)$$

$$= \begin{pmatrix} e^{\lambda t} & t e^{\lambda t} \\ 0 & e^{\lambda t} \end{pmatrix}.$$

The orbits therefore become

$$\gamma(\mathbf{b}) = \left\{ \begin{pmatrix} e^{\lambda t} b_1 + t e^{\lambda t} b_2 \\ e^{\lambda t} b_2 \end{pmatrix}; t \in \mathbb{R} \right\}. \quad (1.2.15)$$

To visualize and plot them on a $y_1 y_2$ -plane, we solve the simultaneous equations,

$$\begin{aligned} y_1 &= e^{\lambda t} b_1 + t e^{\lambda t} b_2, \\ y_2 &= e^{\lambda t} b_2 \end{aligned} \quad (1.2.16)$$

to get

$$\begin{aligned} y_1 &= y_2 \left[\frac{b_1}{b_2} + \frac{1}{\lambda} \ln \left(\frac{y_1}{y_2} \right) \right], \quad \text{if } b_2 \neq 0; \\ y_2 &= 0, y_1 \text{ arbitrary}, \quad \text{if } b_2 = 0. \end{aligned} \quad (1.2.17)$$

We now plot the phase plane for different values of λ and find the following results.

1. When $\lambda \neq 0$, we have a *Jordan node*. For $\lambda < 0$ ($\lambda > 0$), it is *attracting* (*repelling*). **Figure 1.2.6** shows the relevant phase portrait without arrows.
 2. When $\lambda = 0$, we have a *neutral line*. **Figure 1.2.7** shows the relevant phase portrait.
- **Case 3.** The DE can be written as the following set of simultaneous equations:

$$\begin{aligned} \dot{y}_1 &= \alpha y_1 + \beta y_2, \\ \dot{y}_2 &= -\beta y_1 + \alpha y_2. \end{aligned} \quad (1.2.18)$$

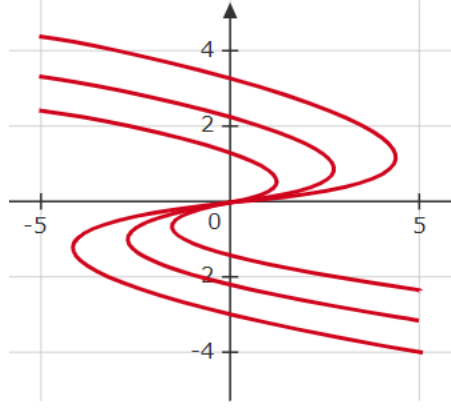


Figure 1.2.6: Phase portrait for a Jordan node.

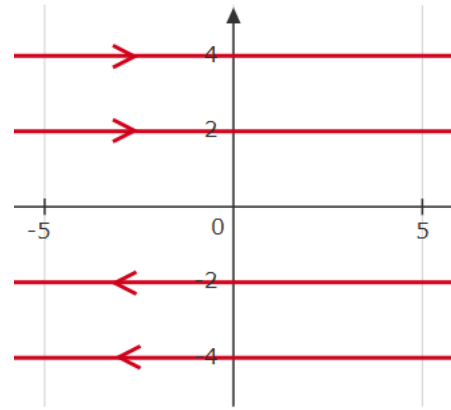


Figure 1.2.7: Phase portrait for a neutral line.

Using polar coordinates where $y_1 = r \cos \theta$ and $y_2 = r \sin \theta$, the DE becomes

$$\begin{aligned} \dot{r} \cos \theta - r \dot{\theta} \sin \theta &= \alpha r \cos \theta + \beta r \sin \theta, \\ \dot{r} \sin \theta + r \dot{\theta} \cos \theta &= -\beta r \cos \theta + \alpha r \sin \theta. \end{aligned} \quad (1.2.19)$$

Solving these simultaneously to get equations for \dot{r} and $\dot{\theta}$, we get

$$\begin{aligned} \dot{r} &= \alpha r, \\ \dot{\theta} &= -\beta. \end{aligned} \quad (1.2.20)$$

Solving these for r and θ , we get the following orbits:

$$\gamma(\mathbf{b}) = \left\{ \begin{pmatrix} r \\ \theta \end{pmatrix} = \begin{pmatrix} e^{\alpha t} r_0 \\ -\beta \theta_0 t \end{pmatrix}; t \in \mathbb{R} \right\}, \quad (1.2.21)$$

where the initial state $\mathbf{b} = (r_0, \theta_0)$ is written in polar coordinates. To visualize and plot these orbits on a $y_1 y_2$ -plane, we solve the simultaneous equations to get

$$r = r_0 \exp \left[-\frac{\alpha}{\beta} (\theta - \theta_0) \right]. \quad (1.2.22)$$

We now plot the phase plane for different values of α (assuming that $\beta > 0$ – the sign of β compared to α will tell us whether the rotation is clockwise or anti-clockwise) and find the following results.

1. When $\alpha \neq 0$, we have a *spiral*. For $\alpha < 0$ ($\alpha > 0$), it is *attracting* (*repelling*).

Figure 1.2.8 shows the relevant phase portrait without arrows.

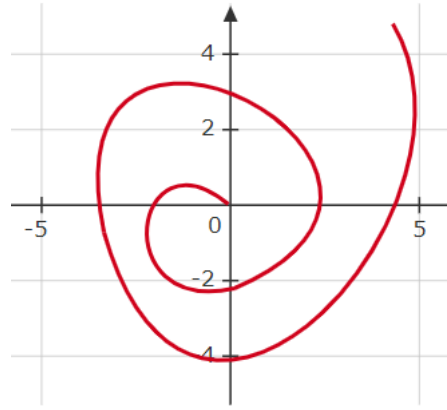


Figure 1.2.8: Phase portrait for a spiral.

2. When $\alpha = 0$, we have a *center*. Refer back to Figure 1.2.1 for the typical phase portrait.

We now have a full characterization of two-dimensional linear systems. To construct the phase portrait for any such system as described by eq. (1.2.1), we can perform the following steps:

1. Find the Jordan canonical form of A .
2. Choose the relevant phase portrait for $\mathbf{y} = J\mathbf{x}$.
3. Use eq. (1.2.7) to transform the axes of this portrait to the one we require.

1.3 Tackling Non-Linear Systems

In the previous section, we looked at linear systems with the intention that non-linear systems can be linearized to learn about their characteristics. The term $DF(\mathbf{x}^*)$ in eq. (1.1.9) is the Jacobian of \mathbf{F} and for two-dimensional systems, can be written as

$$DF(\mathbf{x}^*) = \begin{pmatrix} \frac{\partial F_1}{\partial x_1} & \frac{\partial F_1}{\partial x_2} \\ \frac{\partial F_2}{\partial x_1} & \frac{\partial F_2}{\partial x_2} \end{pmatrix} \bigg|_{\mathbf{x}=\mathbf{x}^*}, \quad (1.3.1)$$

where the subscripts indicate the components of the vectors $\mathbf{F} = (F_1, F_2)$ and $\mathbf{x} = (x_1, x_2)$. To proceed further, we need to introduce the concept of *topological equivalence*. Roughly speaking, two DEs are topologically equivalent, if we can continuously deform the orbits of either one of them to look exactly like the other's. We state here the precise definition for completeness.

Definition 1.3.1 (Topological Equivalence). Two DEs with functions \mathbf{F} and \mathbf{G} are called topologically equivalent if there exists a homeomorphism (i.e. a continuous bijection) \mathbf{H} such that $\mathbf{H} \circ \mathbf{F} = \mathbf{G} \circ \mathbf{H}$.

Looking at the phase portraits in the previous section does give us an idea of which of the DEs might be topologically equivalent to each other. More to the point, if we treat the non-linear system as a perturbation of the linear system, we observe topological equivalence might break. In particular, we can see intuitively that a small perturbation to a center will cause the circles to break down. These ideas are captured by the Hartman-Grobman Theorem. Before, we state it, we need one more definition.

Definition 1.3.2 (Hyperbolic Fixed Point). A fixed point of a linear DE is called hyperbolic if the real part of the eigenvalues of the matrix are non-zero.

We are now in a position to state the theorem.

Theorem 1.3.1 (Hartman-Grobman). *Let \mathbf{F} be continuously differentiable and let \mathbf{x}^* be a hyperbolic fixed point of \mathbf{F} . Then, there exists a neighbourhood U of \mathbf{x}^* such that \mathbf{F} on U is topologically equivalent to its linearization J .*

There seems like a lot to unpick here. However, all of it boils down to checking which of the canonical linear flows have hyperbolic fixed points. A cursory glance through the previous section reveals that these are saddles, nodes, foci and spirals. Therefore, it is these fixed points for which the linearization prediction is accurate. Centers, on the other hand, are not hyperbolic and therefore, even if the linearization predicts a center, the non-linear DE might not have one. Example 1.3.1

Example 1.3.1. Consider the non-linear dynamical system,

$$\begin{aligned} \dot{x}_1 &= -x_2 + x_1(x_1^2 + x_2^2), \\ \dot{x}_2 &= x_1 + x_2(x_1^2 + x_2^2). \end{aligned} \tag{1.3.2}$$

It is easy to see that the origin is a fixed point of the system. To understand the behaviour around the origin, we first use linearization. The Jacobian becomes

$$\begin{aligned} J &= \begin{pmatrix} 3x_1^2 + x_2^2 & -1 + 2x_1x_2 \\ 1 + 2x_1x_2 & x_1^2 + 3x_2^2 \end{pmatrix} \bigg|_{x_1=0, x_2=0}, \\ &= \begin{pmatrix} 0 & -1 \\ 1 & 0 \end{pmatrix} \end{aligned} \tag{1.3.3}$$

Comparing with the canonical linear flows, we find that this predicts a center. However, solving the actual non-linear system and plotting the resultant phase portrait, shows that the origin is actually a spiral. This is in accordance with what the Hartman-Grobman Theorem tells us.

Linearization therefore presents one useful way of looking at non-linear systems. We now look for other methods to find out characteristics of some particular types of

non-linear systems. One of these types is the *conservative system*. As the name suggests, it is a system which possesses a quantity that is conserved in time. We shall use the following precise definition for a conserved quantity.

Definition 1.3.3 (Conserved Quantity). A conserved quantity is a real-valued continuous function $E(\mathbf{x})$ which is constant on all orbits of the system but is non-constant on every open set in phase space.

The second condition is necessary to ensure that the conserved quantity does not stay constant for all states of the system. We can now describe some characteristics of conservative systems.

1. A conservative system cannot have any attracting fixed points. To prove this, assume on the contrary, that there does exist an attracting fixed point \mathbf{x}^* and a conserved quantity $E(\mathbf{x})$. Then, there exists an open set \mathcal{B} (the *basin of attraction*) of orbits in phase space all of which are attracted to the fixed point. Then, since $E(\mathbf{x})$ is constant on all orbits, and each of them ends in \mathbf{x}^* , then $E(\mathbf{x}) = E(\mathbf{x}^*)$ in \mathcal{B} . But a conserved quantity must be non-constant on every open set in phase space. Therefore, we have a contradiction.
2. All orbits sufficiently close to an isolated fixed point of a conservative system are closed if the fixed point is a local minimum of the conserved quantity. This property can be seen in [Figure 1.3.1](#). Since $E(\mathbf{x})$ is constant on orbits, the orbits must lie in contours of $E(\mathbf{x})$. Since the contours are closed and contain no fixed points (by the isolation of the fixed point in consideration), the orbit must consist of the whole contour and should thus be closed. In particular, for a conservative system, if the linearization predicts a center and the fixed point is isolated, the non-linear system does indeed have a center. See [Example 1.3.2](#) for an illustration.

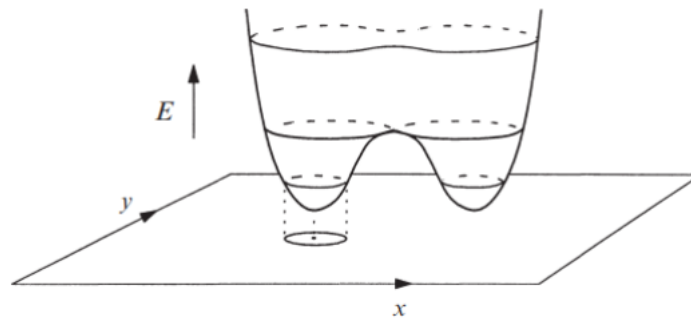


Figure 1.3.1: Closed orbits in a conservative system.

Example 1.3.2. Consider a particle of mass $m = 1$ moving in a one-dimensional potential

$$V(x) = -\frac{1}{2}x^2 + \frac{1}{4}x^4. \quad (1.3.4)$$

Using $F = ma$, where $F = -\frac{dV}{dx}$ and $a = \ddot{x}$,

$$\ddot{x} = x - x^3 \quad (1.3.5)$$

By introducing the velocity $v = \dot{x}$, we can rewrite eq. (1.3.5) as a dynamical system:

$$\begin{aligned} \dot{x} &= v, \\ \dot{v} &= x - x^3. \end{aligned} \quad (1.3.6)$$

This is a conservative system because the total energy $E(x) = K + V = \frac{1}{2}v^2 - \frac{1}{2}x^2 + \frac{1}{4}x^4$ must remain constant. Using $(\dot{x}, \dot{v}) = (0, 0)$, we find the fixed points of the system to be $(0, 0)$, $(1, 0)$ and $(-1, 0)$. The linearization at each of the fixed points can be calculated and found to be

$$J_{(0,0)} = \begin{pmatrix} 0 & 1 \\ 1 & 0 \end{pmatrix}, \quad J_{(1,0)} = \begin{pmatrix} 0 & 1 \\ -2 & 0 \end{pmatrix}, \quad J_{(-1,0)} = \begin{pmatrix} 0 & 1 \\ -2 & 0 \end{pmatrix} \quad (1.3.7)$$

After computing the relevant Jordan forms, we find that $(0, 0)$ is predicted to be a saddle while $(\pm 1, 0)$ are both predicted to be centers. Since this is a conservative system, a numerically constructed phase portrait of the system will reveal the same.

Another type of non-linear systems is a *reversible system*. This is a system which remains unchanged under the simultaneous transformations $x_2 \rightarrow -x_2$ and $t \rightarrow -t$. In other words, the phase portrait of the system has reflection across the x_1 -axis as a symmetry of the system, provided that the direction of the arrows above and below the plane is opposite. A very important property of reversible systems (which we state without proof) is that if linearization predicts a center at the origin for the system, the full non-linear system also has a center at the origin. A way to employ this useful tool is shown in Example 1.3.3.

Example 1.3.3. Consider the two-dimensional nonlinear dynamical system,

$$\begin{aligned} \dot{x}_1 &= x_2 - x_2^3, \\ \dot{x}_2 &= -x_1 - x_2^2 \end{aligned} \quad (1.3.8)$$

To check whether the system is reversible, we apply the transformations to get

$$\begin{aligned} -\dot{x}_1 &= -x_2 - (-x_2)^3, \\ \dot{x}_2 &= -x_1 - (-x_2)^2. \end{aligned} \quad (1.3.9)$$

These are the same as the previous equations. Therefore, the system is reversible. We can clearly see that the origin is a fixed point of the system. Calculating the linearization yields:

$$J = \left. \begin{pmatrix} 0 & 1 - 3x_2^2 \\ -1 & -2x_2 \end{pmatrix} \right|_{x_1=0, x_2=0} = \begin{pmatrix} 0 & 1 \\ -1 & 0 \end{pmatrix}. \quad (1.3.10)$$

The linearization predicts a center. Therefore, the full non-linear system also has a center at the origin. This is confirmed by the numerically generated phase portrait for the system shown in [Figure 1.3.2](#).

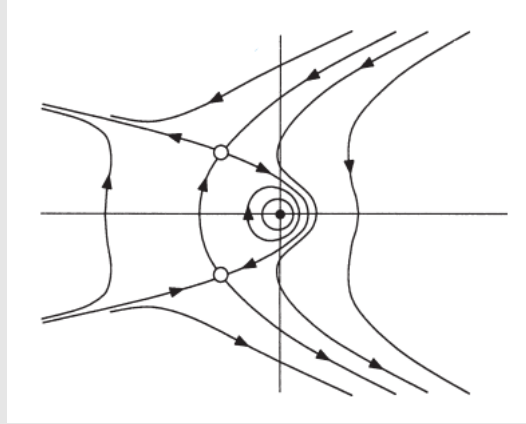


Figure 1.3.2: Phase portrait for a nonlinear reversible system with a center at the origin.

While the previous techniques have been helpful in establishing closed orbits for certain systems, nonlinear systems are not always reversible or conservative. We shall now look at techniques to establish when systems do not have closed orbits.

A dynamical system is called a *gradient system* if it can be written as

$$\dot{\mathbf{x}} = -\nabla V(\mathbf{x}), \quad (1.3.11)$$

where $V(\mathbf{x})$ is a real-valued scalar function which we shall call a potential. Gradient systems do not have closed orbits. To prove this, assume on the contrary that a closed orbit exists. Then, the change in the potential ΔV around that orbit must be zero. But we can calculate this change in the following way as well:

$$\begin{aligned} \Delta V &= \int_0^T dt \frac{dV}{dt}, \\ &= \int_0^T dt \left(\frac{\partial V}{\partial x_1} \frac{dx_1}{dt} + \dots + \frac{\partial V}{\partial x_n} \frac{dx_n}{dt} \right), \\ &= \int_0^T dt \nabla V \cdot \dot{\mathbf{x}}, \\ &= \int_0^T dt (-\dot{\mathbf{x}}) \cdot \dot{\mathbf{x}}, \\ &= - \int_0^T dt |\dot{\mathbf{x}}|^2, \\ &< 0. \end{aligned} \quad (1.3.12)$$

Here, T is the time taken to complete the orbit. Since we have a contradiction at the end, we conclude that gradient systems cannot have closed orbits.

Next, if the system allows a *Liapunov function*, it cannot contain closed orbits. A Liapunov function is defined as a continuously differentiable, real-valued function $V(\mathbf{x})$ such that

1. $V(\mathbf{x}) > 0$ for all $\mathbf{x} \neq \mathbf{x}^*$ and $V(\mathbf{x}^*) = 0$,
2. $\dot{V}(\mathbf{x}) = 0$ for all $\mathbf{x} \neq \mathbf{x}^*$.

Here, as always, \mathbf{x}^* is a fixed point. Since $V(\mathbf{x})$ is decreasing on all orbits and bounded from below by 0 at the fixed point, we have that all orbits will end at the fixed point and there can be no closed orbits. See Example 1.3.4 for an example of a Liapunov function.

Example 1.3.4. Consider the dynamical system,

$$\begin{aligned} \dot{x}_1 &= -x_1 + 4x_2, \\ \dot{x}_2 &= -x_1 - x_2^3. \end{aligned} \tag{1.3.13}$$

Let $V(x_1, x_2) = x_1^2 + 4x_2^2$. Clearly, $V(x_1, x_2) > 0$ everywhere except at the origin which is a fixed point. There, $V(0, 0) = 0$. Differentiating w.r.t. t , we get

$$\begin{aligned} \dot{V}(x_1, x_2) &= 2x_1\dot{x}_1 + 8x_2\dot{x}_2, \\ &= 2x_1(-x_1 + 4x_2) + 8x_2(-x_1 - x_2^3), \\ &= -2x_1^2 - 8x_2^4. \end{aligned} \tag{1.3.14}$$

Clearly, $\dot{V} < 0$ everywhere except the origin. Therefore, $V(x_1, x_2)$ is a Liapunov function for this dynamical system. Hence, it has no closed orbits.

Another strategy to establish whether a system has no closed orbits is *Dulac's criterion*. Similar to finding a Liapunov function, here we assume that a continuously differentiable real-valued function $g(\mathbf{x})$ exists such that $\nabla \cdot (g\dot{\mathbf{x}})$ is either positive or negative everywhere in a simply connected region². To prove that no closed orbits exist in this region for such a system, once again, we assume on the contrary that a closed orbit exists. Then, applying Green's Theorem to the function $g\dot{\mathbf{x}}$ on the closed orbit, we get

$$\iint_S dA \nabla \cdot (g\dot{\mathbf{x}}) = \oint_C dl g\dot{\mathbf{x}} \cdot \hat{\mathbf{n}}. \tag{1.3.15}$$

Here, S represents the surface enclosed by the closed orbit and $\hat{\mathbf{n}}$ is the outward normal vector to the orbit curve C . Now, since $\nabla \cdot (g\dot{\mathbf{x}})$ has only one sign throughout, the left-hand side of eq. (1.3.15) must be non-zero. On the other hand, since $\dot{\mathbf{x}}$ is tangent to orbits $\dot{\mathbf{x}} \cdot \hat{\mathbf{n}} = 0$ causing the right-hand side to be zero. This is a contradiction. Take a look at Example 1.3.5 for an implementation of Dulac's criterion.

Example 1.3.5. Consider the two-dimensional dynamical system,

² Any two points in the region can be joined by a continuous line.

$$\begin{aligned} \dot{x}_1 &= x_1(2 - x_1 - x_2), \\ \dot{x}_2 &= x_2(4x_1 - x_1^2 - 3). \end{aligned} \quad (1.3.16)$$

Let us take $g(x_1, x_2) = \frac{1}{x_1 x_2}$. Then,

$$\begin{aligned} \nabla \cdot (g\dot{\mathbf{x}}) &= \frac{\partial}{\partial x_1} \left(\frac{x_1(2 - x_1 - x_2)}{x_1 x_2} \right) + \frac{\partial}{\partial x_2} \left(\frac{x_2(4x_1 - x_1^2 - 3)}{x_1 x_2} \right), \\ &= -\frac{1}{x_2}. \end{aligned} \quad (1.3.17)$$

This is negative throughout the simply connected region $x_1 > 0, x_2 > 0$ i.e. the first quadrant. Therefore, by Dulac's criterion, there can be no closed orbits in the first quadrant.

Both the Liapunov function method and Dulac's criterion have the drawback that they do not give a procedure to find such functions. In both examples, we stumbled upon these functions by pure luck.

We end this discussion of non-linear systems with arguably the most important theorem in the theory of two-dimensional dynamical systems. The past three methods have focused on eliminating the possibility of closed orbits. We shall now discuss a method to prove the existence of closed orbits based on the Poincaré-Bendixson Theorem which we state here without proof.

Theorem 1.3.2 (Poincaré-Bendixson Theorem). *Let C be an orbit that stays in a closed, bounded subset of the plane denoted by R . Then, either C is closed or it spirals towards a closed orbit as $t \rightarrow \infty$.*

The important criterion here is that C must stay in R for all time t . One way to ensure this is to construct a trapping region as shown in Figure 1.3.3. The specifics of such a construction are illustrated in Example 1.3.6.

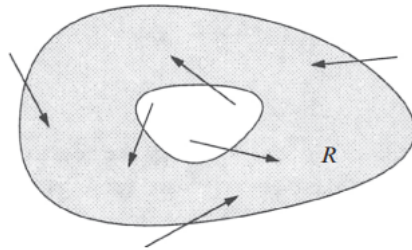


Figure 1.3.3: Trapping region to apply the Poincaré-Bendixson Theorem.

Example 1.3.6. Consider the dynamical system defined using polar coordinates:

$$\begin{aligned}\dot{r} &= r(1 - r^2) + 0.5r \cos \theta, \\ \dot{\theta} &= 1.\end{aligned}\tag{1.3.18}$$

We shall construct an annulus as a trapping region R with $\dot{r} < 0$ on the outer boundary and $\dot{r} > 0$ on the inner boundary so that any orbit remains trapped inside R . There are no fixed points inside R since $\dot{\theta} \neq 0$ anywhere. Let the inner boundary be defined by r_{\min} and the outer boundary by r_{\max} . Then, to find r_{\min} , we must have $\dot{r} = r(1 - r^2) + 0.5r \cos \theta > 0$. Since $\cos \theta \geq -1$, we get $r_{\min}(1 - r_{\min}^2) - 0.5r_{\min} > 0$. Solving for r_{\min} yields

$$r_{\min} < \sqrt{0.5}.\tag{1.3.19}$$

Noting that $\cos \theta < 1$, a similar calculation for r_{\max} yields

$$r_{\max} > \sqrt{1.5}.\tag{1.3.20}$$

In particular, if we define our region by $\sqrt{0.5} < r < \sqrt{1.5}$, the Poincaré-Bendixson Theorem tells us that a closed orbit must exist inside this region.

THE BIANCHI IX UNIVERSE

Our universe is homogeneous and isotropic on large scales according to the Cosmic Microwave Background (CMB) which is the earliest experimental evidence we currently possess. Before this time, nearer to the initial singularity (or the Big Bang as it is commonly known), there is no experimental evidence to suggest that homogeneity and isotropy persists. Assuming homogeneity but foregoing isotropy seems like a step in the right direction if one wants to explore solutions to the Einstein Field Equations (EFEs) near the initial singularity. To this end, Bianchi, Taub and Ellis and MacCallum among others put forth a complete classification of all homogeneous cosmologies. The Bianchi IX universe is the ninth and last cosmological model in their list.

2.1 The Metric and Some Calculations

The Bianchi IX universe is a homogeneous, anisotropic cosmological model characterized by the following diagonalized metric:

$$ds^2 = -dt^2 + \sum_{k=1}^3 (l_k)^2 \sigma_k^2. \quad (2.1.1)$$

Let us begin to unpick this equation. The metric signature is $(-, +, +, +)$ as is usual in cosmology. The time component is the same as in the Friedmann-Lemaître-Robertson-Walker (FLRW) metric. The changes are in the spatial components. Instead of being

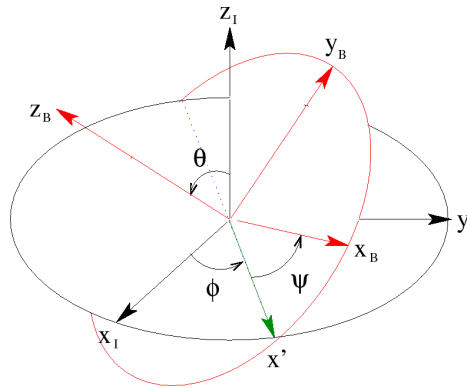


Figure 2.1.1: A depiction of Euler angles.

diagonalized along the usual x, y and z directions, the metric is diagonalized along these weird σ_1, σ_2 and σ_3 directions, which can be written in terms of Euler angle coordinates (ψ, θ, ϕ) as

$$\begin{aligned}\sigma_1 &= (0, \sin \psi, -\cos \psi \sin \theta), \\ \sigma_2 &= (0, \cos \psi, \sin \psi \sin \theta), \\ \sigma_3 &= (-1, 0, \cos \theta).\end{aligned}\tag{2.1.2}$$

Here, the ranges for each Euler angle are $0 \leq \psi \leq 4\pi$, $0 \leq \theta \leq \pi$, $0 \leq \phi \leq 2\pi$. See [Figure 2.1.1](#) for a visualization. The l_k 's correspond to three different scale factors which we shall relabel as $a(t)$, $b(t)$ and $c(t)$ from now on. Therefore, the universe is expanding and/or contracting according to these scale factors along three different directions.

We now find the spatial volume of the universe at any given time in these coordinates:

$$\begin{aligned}V &= \iiint \sqrt{a^2 b^2 c^2} \sigma_1 \wedge \sigma_2 \wedge \sigma_3, \\ &= abc \iiint [-\sin^2 \psi \sin \theta (d\theta \wedge d\phi \wedge d\psi) + \cos^2 \psi \sin \theta (d\phi \wedge d\theta \wedge d\psi)], \\ &= abc \iiint [\sin^2 \psi \sin \theta (d\phi \wedge d\theta \wedge d\psi) + \cos^2 \psi \sin \theta (d\phi \wedge d\theta \wedge d\psi)], \\ &= abc \iiint \sin \theta (d\phi \wedge d\theta \wedge d\psi), \\ &= abc \int_0^{4\pi} d\psi \int_0^\pi \sin \theta d\theta \int_0^{2\pi} d\phi, \\ &= 16\pi^2 abc.\end{aligned}\tag{2.1.3}$$

Here, we have used standard properties of the wedge product of two differential forms to reach our answer. This calculation shows that the Bianchi IX universe has closed spatial sections with finite volume since the scale factors are finite.

We can now use the metric in the vacuum EFEs (assuming a zero cosmological constant) to find the evolution equations for the scale factors. Before this, we introduce a new time coordinate τ defined by

$$dt = abc d\tau.\tag{2.1.4}$$

Usually, $abc \sim t$ so that $\tau \sim \ln t$ and therefore, the initial singularity at $t = 0$ is at $\tau = -\infty$. With this change in coordinate, the evolution equations become

$$\frac{d^2}{d\tau^2}(\ln a^2) = (b^2 - c^2)^2 - a^4,\tag{2.1.5}$$

and cyclically, $a \rightarrow b \rightarrow c \rightarrow a$. These equations are intractable analytically. We therefore look for approximations to these equations which preserve the behaviour near the singularity.

2.2 The BKL Approximation

The Belinski-Khalatnikov-Lifshitz (BKL) approximation to the Bianchi IX behaviour was developed by Belinski, Khalatnikov and Lifshitz while they were at the Landau Institute for Theoretical Physics. To understand it, we first need to take a look at the Bianchi I metric:

$$ds^2 = -dt^2 + \sum_{k=1}^3 (l_k)^2 dx_k^2. \quad (2.2.1)$$

The Kasner solution to the Bianchi I universe involves writing down the scale factors as powers of t :

$$ds^2 = -dt^2 + \sum_{k=1}^3 t^{2p_k} dx_k^2. \quad (2.2.2)$$

The p_k 's satisfy the two constraints,

$$\sum_{k=1}^3 p_k = \sum_{k=1}^3 p_k^2 = 1 \quad (2.2.3)$$

and we can choose the numbering of the indices such that

$$-\frac{1}{3} \leq p_1 \leq 0 \leq p_2 \leq \frac{2}{3} \leq p_3 \leq 1. \quad (2.2.4)$$

This latter result shows that the Kasner universe expands in one direction and contracts in the other two as we evolve towards the initial singularity ($t \rightarrow 0$). Now, BKL used the constraints in eq. (2.2.3) to express the p_k 's in terms of a single parameter u – the so-called BKL parameter. The definition of each index in terms of u becomes

$$\begin{aligned} p_1 &= -\frac{u}{u^2 + u + 1}, \\ p_2 &= \frac{u + 1}{u^2 + u + 1}, \\ p_3 &= \frac{u(u + 1)}{u^2 + u + 1}. \end{aligned} \quad (2.2.5)$$

But this has just been a description of Bianchi I so far. To describe Bianchi IX, BKL approximate this universe by a series of Kasner epochs. During each epoch, u evolves according to the EFEs obtained by using the metric given in eq. (2.2.2). Between epochs, u evolves according to the *Gauss map*,

$$u_{n+1} = \begin{cases} u_n - 1 & u_n > 1, \\ \frac{1}{u_n} & u_n < 1. \end{cases} \quad (2.2.6)$$

Numerical solutions to the full behaviour as encoded in eq. (2.1.5) have shown that the BKL approximation is very accurate close to the initial singularity.

2.3 The Hamiltonian Formulation

At around the time that BKL were developing their approximation, Charles Misner developed a Hamiltonian formulation for the Bianchi IX universe. He did this by introducing the minisuperspace (MSS) variables $(\Omega, \beta_+, \beta_-)$. These are defined in terms of the scale factors a, b and c by

$$\begin{aligned}\Omega &= -\frac{1}{3} \ln(abc), \\ \beta_+ &= -\ln \left[\frac{c}{(abc)^{1/3}} \right], \\ \beta_- &= \frac{1}{\sqrt{3}} \ln \left(\frac{a}{b} \right).\end{aligned}\tag{2.3.1}$$

It is easy to check by comparing with eq. (2.1.3) that in these coordinates, the volume is given by $V = 16\pi^2 e^{-3\Omega}$. Therefore, Ω quantifies the volume of the universe whereas the shape parameters β_+ and β_- describe the anisotropy of the universe. One can describe the evolution of this universe by giving its shape as a function of its volume, thereby treating Ω , in effect, as a time parameter. Using the Arnowitt-Deser-Misner (ADM) formulation of General Relativity (GR), we can write a Hamiltonian for this system,

$$H^2 = p_+^2 + p_-^2 + e^{-4\Omega}(V - 1),\tag{2.3.2}$$

where the anisotropy potential V is

$$V(\beta_+, \beta_-) = \frac{1}{3}e^{-8\beta_+} - \frac{4}{3}e^{-2\beta_+} \cosh(2\sqrt{3}\beta_-) + 1 + \frac{2}{3}e^{4\beta_+}[\cosh(4\sqrt{3}\beta_-) - 1].\tag{2.3.3}$$

The p 's in eq. (2.3.3) are the conjugate momenta for the β 's. Since we are treating Ω as a time-coordinate, we have a two-dimensional phase space, the $\beta_+\beta_-$ -plane where the dynamics is happening. In this plane, V is symmetric under rotations by $\frac{2\pi}{3}$ which are the symmetries of an equilateral triangle, thereby indicating that equipotentials should be equilateral triangles in this plane. The evolution of the universe can now be described by a phase point in this plane interacting with the potential walls.

INDICATORS OF CHAOS

Chaotic phenomena abound in nature. From turbulent water flows to cardiac arrhythmias, from the double pendulum to population models based on the logistic map, chaos seems to arise almost everywhere. In fact, it may not be a stretch to say that it is difficult to find macroscopic systems in nature where there is no propensity for chaos. Therefore, with chaos so rampant in nature, where better to look for it than in the most non-linear theory of them all - GR. In this chapter, we shall look at indicators of chaos and attempt to apply them to the Bianchi IX universe as a toy model to show that the EFEs admit chaotic solutions.

3.1 What is Chaos?

In [Chapter 1](#), we learned about various kinds of behaviour around the fixed points of a dynamical system. We also noted that "chaos" cannot exist in two-dimensional dynamical systems. But we stopped short of defining chaos. The behaviour that we studied could broadly be divided into two categories: periodic and non-periodic. It is reasonable to expect that periodic behaviour cannot produce the richness that chaos demands. Therefore, chaos must be non-periodic. Furthermore, as is apparent from one of the more popular versions of chaos – the "butterfly effect" whence the fluttering of a butterfly's wings in Brazil can cause a tornado in the United States – there must exist an element of unpredictability in chaos. Combining all of this gives us the following precise definition:

Definition 3.1.1 (Chaos). Chaos is aperiodic long-term behaviour in a deterministic system that exhibits sensitive dependence on initial conditions.

Suppose we have knowledge of initial conditions albeit with a slight uncertainty for a chaotic system. Then, the long-term behaviour of the system cannot be predicted despite being described by deterministic equations.

The aforementioned description of chaos and the general theory of non-linear dynamical systems that we have developed so far relies crucially on an independent choice of the time coordinate. Everything else is measured against this time. In GR,

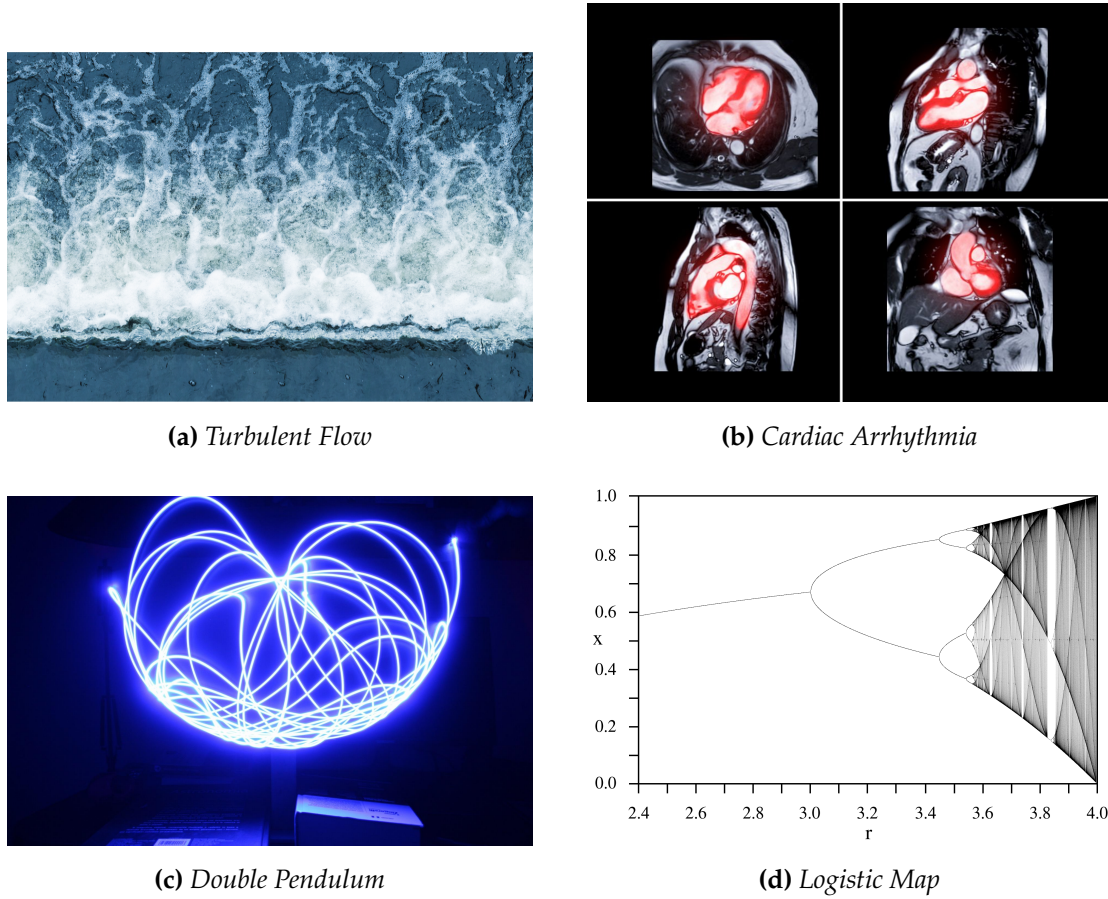


Figure 3.1.1: *Chaos abounds in nature.*

however, there is no way of choosing a particular time coordinate. Any choice is valid since the theory is invariant under spacetime diffeomorphisms. We are thus presented with a problem. How can we categorize and even define chaos in a coordinate-invariant manner? In the following sections, we shall look at a few indicators of chaos. They are, by no means, a guarantee for the presence of chaos but their presence makes chaos highly probable.

3.2 Painlevé Test

A DE is called integrable if it has enough first integrals giving us global knowledge of its general solution. In our context, it is important to realize that an integrable system cannot be chaotic. The converse, however, is not true. Regardless, if we can find a way to establish whether a system in GR is integrable, we can eliminate the possibility of chaos. One way to do this is the *Painlevé test*. A system which passes the Painlevé test is said to possess the Painlevé property (PP). A precise definition of the PP follows.

Definition 3.2.1 (Painlevé property (PP)). A DE is said to possess the PP if the only movable singularities in its general solution are poles.

Let us unpick this definition. The general solution of a DE is a solution with as many

arbitrary constants (to be specified by giving initial conditions or boundary values) as the order of the DE. A movable singularity in the general solution is one whose location in the complex plane depends on the arbitrary constants – it can "move" by changing the value of these constants. See Example 3.2.1 for one such example.

Example 3.2.1. Consider the DE,

$$\frac{du}{dx} + \frac{u^2}{x} = 0. \quad (3.2.1)$$

Since the order of the DE is 1, we need to find a general solution with 1 arbitrary constant. Let $u(x) = \frac{1}{c + \ln x}$, where c is an arbitrary constant. Then,

$$\frac{du}{dx} = -\frac{1}{x(c + \ln x)^2}, \quad (3.2.2)$$

and

$$\frac{u^2}{x} = \frac{1}{x(c + \ln x)^2}. \quad (3.2.3)$$

Therefore, a general solution for the DE is

$$u(x) = \frac{1}{c + \ln x}. \quad (3.2.4)$$

It can be readily checked that this has a singularity at $x = e^{-c}$. Furthermore, this singularity is a pole (in the usual complex analysis meaning of the term) and it is movable (it depends on the value of the arbitrary constant c). Therefore, the DE in eq. (3.2.1) has the PP.

Contopoulos, Grammaticos and Ramani and separately, Latifi, Musette and Conte performed a Painlevé test for the Bianchi IX universe. They found that there exists an essential movable singularity in the general solution. Therefore, the Bianchi IX universe does not possess the PP and is therefore not integrable. This increases the likelihood of (but does not confirm) the existence of chaos in the system.

3.3 Kolmogorov-Sinai (KS) Entropy for Discrete Maps

A way to quantify chaos in GR is by approximating the full system by a discrete map and exploring the possibility of chaos in the latter. This method does not guarantee the existence of chaos in the full system but due to the very well-developed theory of discrete-time dynamical systems (including ergodic theory), it does guarantee the existence of chaos in the discrete approximation. Luckily, we have an excellent discrete approximation of the Bianchi IX universe – the BKL approximation. Before diving into it, we develop some theory for discrete maps.

Consider a discrete map $T : [0, 1] \rightarrow [0, 1]$. The Kolmogorov-Sinai (KS) entropy gives us a way to quantify the chaos that exists in the map. Consider an ensemble of orbits. Let Δ_t denote the distance between two orbits in the ensemble at time t . Then,

the KS entropy h of the map is given by

$$h = \frac{\langle \ln(\Delta_t/\Delta_0) \rangle}{t}. \quad (3.3.1)$$

The interpretation is that a positive h represents a sensitive dependence on initial conditions as orbits in the ensemble move away from each other on average. This indicates that an initial uncertainty would grow exponentially over time. Using results from measure theory, we can rewrite h in a more calculation-friendly way,

$$h = \int_0^1 \ln |T'(x)| \mu(x) dx, \quad (3.3.2)$$

where the prime over T indicates a derivative w.r.t. x . Here, $\mu(x)$ is an invariant measure¹ preserved by T i.e.

$$\mu(T^{-1}A) = \mu(A), \quad (3.3.3)$$

for all sets A in the domain of T .

Now, the BKL approximation to the Bianchi IX universe has the following form upon restricting the domain to $[0, 1]$:

$$T(x) = \frac{1}{x} - k; \quad \frac{1}{k+1} < x < \frac{1}{k}, \quad (3.3.4)$$

where k is a positive integer. We can see from the form of eq. (3.3.4) that every $x \in [0, 1]$ has an infinite number of pre-images, one in each interval $[\frac{1}{k+1}, \frac{1}{k}]$. Then, if we consider an open interval $A = (a, b) \in [0, 1]$, the pre-images of A can be seen to lie in an infinite union of disjoint intervals of the form

$$T^{-1}(a, b) = \cup_{n=1}^{\infty} \left(\frac{1}{n+b}, \frac{1}{n+a} \right). \quad (3.3.5)$$

From elementary measure theory, note that

$$\mu(A) = \int_a^b \mu(x) dx. \quad (3.3.6)$$

Using this and noting that the measure μ is additive (i.e. $\mu(A \cup B) = \mu(A) + \mu(B)$ if A and B are disjoint), we get

$$\mu(T^{-1}A) = \sum_{n=1}^{\infty} \int_{1/(n+b)}^{1/(n+a)} \mu(x) dx. \quad (3.3.7)$$

For T to be measure-preserving, we require the equality of eqs. (3.3.6) and (3.3.7). Let us guess a solution, namely $\mu(x) = \frac{1}{(1+x)\ln 2}$ and check whether it satisfies our condition. We get

$$\begin{aligned} \mu(A) &= \int_a^b \frac{1}{(1+x)\ln 2} dx, \\ &= \frac{1}{\ln 2} \ln \left(\frac{1+b}{1+a} \right), \end{aligned} \quad (3.3.8)$$

¹ A measure can be thought of as a tool to determine the size of intervals.

and

$$\begin{aligned}
 \mu(T^{-1}A) &= \sum_{n=1}^{\infty} \int_{1/(n+b)}^{1/(n+a)} \frac{1}{(1+x) \ln 2} dx, \\
 &= \frac{1}{\ln 2} \sum_{n=1}^{\infty} \ln \left[\frac{(n+a+1)(n+b)}{(n+a)(n+b+1)} \right], \\
 &= \frac{1}{\ln 2} \ln \left[\frac{(2+a)(1+b)(3+a)(2+b)}{(1+a)(2+b)(2+a)(3+b)} \cdots \right], \\
 &= \frac{1}{\ln 2} \ln \left(\frac{1+b}{1+a} \right), \\
 &= \mu(A).
 \end{aligned} \tag{3.3.9}$$

Therefore, our guess was right! Now, we use eq. (3.3.4) to find $T'(x)$:

$$T'(x) = -\frac{1}{x^2}. \tag{3.3.10}$$

Since T is measure-preserving and the conditions necessary for eq. (3.3.2) to hold are satisfied, we can find the KS entropy for the BKL approximation:

$$\begin{aligned}
 h &= \int_0^1 \ln \left(\frac{1}{x^2} \right) \frac{1}{(1+x) \ln 2} dx, \\
 &= -\frac{2}{\ln 2} \int_0^1 \frac{\ln x}{x+1} dx, \\
 &= \frac{\pi^2}{6 \ln 2}.
 \end{aligned} \tag{3.3.11}$$

Since $h > 0$, the BKL approximation to the Bianchi IX universe predicts a chaotic solution.

3.4 Liapunov Exponents

The primary way to measure chaos in non-GR applications is via Liapunov exponents. Similar in nature to the KS entropy for discrete maps, the Liapunov exponents quantify how fast orbits move away from each other and therefore, how fast an initial uncertainty grows over time. For an n -dimensional autonomous system with a time parameter that can go up to infinity, the k th Liapunov exponent is defined for an invariant² set in the following way:

$$h_k = \lim_{t \rightarrow \infty} \frac{1}{t} \ln \left(\frac{|\eta_k(t)|}{|\eta_k(0)|} \right), \tag{3.4.1}$$

where $k = 0, \dots, n$ and the η 's are tangent vectors to \mathbf{x} . As was the case with the KS entropy, if the maximal Liapunov exponent $h_{\max} > 0$, then the system is chaotic. As can be seen in eq. (3.4.1), however, there is an explicit reference to a time coordinate and therefore, a reparametrization should lead to a change in the value of the Liapunov

² All orbits that start in the set remain inside the set for all time t .

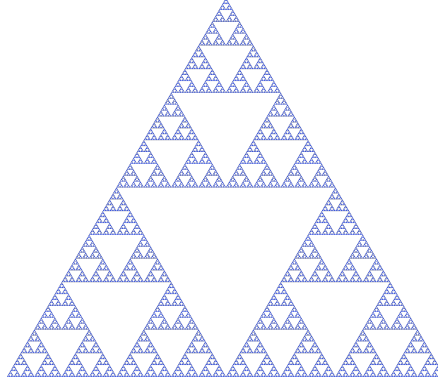


Figure 3.5.1: The Sierpinski Triangle is a fractal.

exponent. Motter, though, has shown that after a reparametrization $\tau(t)$, the Liapunov exponents are rescaled according to the following transformation equation:

$$h_k^\tau = \frac{h_k^t}{\langle \lambda \rangle_t}, \quad (3.4.2)$$

where the superscripts indicate the time coordinate used and $\langle \lambda \rangle_t$ is the average of $\frac{d\tau}{dt}$ over an ensemble of orbits. Despite this result, since Liapunov exponents are only defined for a bounded invariant set, they are not suitable for use for the Bianchi IX universe. This is why numerical solutions have disagreed on the sign of the maximal Liapunov exponent with some finding a positive sign while others finding the exponent to go asymptotically to zero as one approaches the initial singularity.

3.5 Fractals

A fractal is a shape with a self-similar structure (see [Figure 3.5.1](#) for an example). Fractals are associated with chaos in dynamical systems since their extremely detailed nature lends itself readily to the sensitive dependence on initial conditions that chaos demands. With each fractal, we can associate fractal dimensions. Naturally, for fractals, these dimensions have a non-zero fractional part. One example of such a dimension is the *box-counting dimension*. Consider an n -dimensional box of size ϵ . Then, the box-counting dimension D for an object specifies the rate at which the number of boxes N required to cover the object completely increases compared to the rate at which $\epsilon \rightarrow 0$. This can be explained in terms of the formula,

$$D = \lim_{\epsilon \rightarrow 0} \frac{\ln N}{\ln(1/\epsilon)}. \quad (3.5.1)$$

For the irregular area shown in [Figure 3.5.2](#), $N \sim \frac{A}{\epsilon^2}$ where A is the area of the figure. Therefore, $D = 2$ for the object.

To utilize fractals for the study of chaos in GR, we first need to find an invariant set and then set about numerically computing its fractal dimension. Cornish and Levin did this for the Bianchi IX universe and found that there existed a set for which the

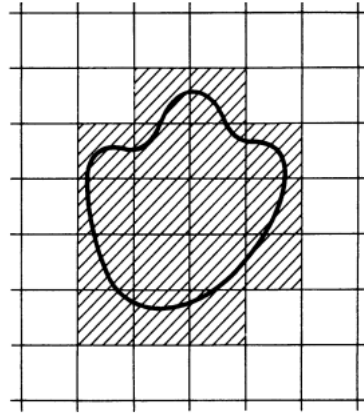


Figure 3.5.2: Schematic of the box-counting dimension for an irregular area.

fractal dimension was 1.72 ± 0.02 which indicates that a fractal exists in the phase space of the model. As with all numerical techniques, though, this result has also not been analytically proven and is therefore, not a guarantor of chaos in the Bianchi IX universe.

A GLIMPSE INTO THE FUTURE

If the Bianchi IX universe is indeed chaotic and experimental evidence is found to support that it describes the universe at the time of the initial singularity, we have a fascinating situation at our hands. For Bianchi IX, chaos means that the universe evolved from completely arbitrary initial conditions. This is because we are running the model backwards in time and conditions today cannot predict conditions at the time of the initial singularity. This amazing conclusion begs us to consider this topic seriously.

To date, the problem of defining and giving a concrete characterization of chaos in GR remains an open problem. Some possible avenues of research are collected here for the reader's convenience:

- The ultimate goal would be Wheeler's dream of geometrodynamics and the superspace – a space where all 3-metrics live and on which we could define a supermetric. This supermetric would then be able to provide us with a concrete definition of distances between metrics, thereby allowing us to compute whether orbits move away from each other under the action of the EFEs. This dream remains far away from reality.
- Another avenue is to define chaos in terms of curvature invariants. A possible way is to use the ADM formulation to write down a Hamiltonian for the system and then use it to define orbits as flows on some manifold. Then, techniques from differential geometry and dynamical systems could be used to relate the curvature of the space with the chaotic nature of its geodesics. An example in this regard is Hopf's work on geodesic flows on surfaces of negative curvature – primarily the hyperbolic plane.
- More specific to the "chaotic cosmology" program as it is called, it is very unlikely that the Bianchi IX universe exactly describes the universe at the time of the initial singularity. The energy scales at the time require quantum mechanics to be taken into account. Therefore, any research into chaos in GR would need to be done in the context of a theory of quantum gravity.

BIBLIOGRAPHY

- Barrow, John D. (1982). "Chaotic behaviour in general relativity". In: *Physics Reports* 85.1, pp. 1–49. ISSN: 0370-1573. DOI: [https://doi.org/10.1016/0370-1573\(82\)90171-5](https://doi.org/10.1016/0370-1573(82)90171-5). URL: <https://www.sciencedirect.com/science/article/pii/0370157382901715>.
- Conte, R. (1997). *The Painlevé approach to nonlinear ordinary differential equations*. arXiv: solv-int/9710020 [solv-int].
- Contopoulos, G, B Grammaticos, and A Ramani (Sept. 1995). "The last remake of the mixmaster universe model". In: *Journal of Physics A: Mathematical and General* 28.18, p. 5313. DOI: [10.1088/0305-4470/28/18/020](https://doi.org/10.1088/0305-4470/28/18/020). URL: <https://dx.doi.org/10.1088/0305-4470/28/18/020>.
- Cornish, Neil J. and Janna J. Levin (June 1997). "Mixmaster universe: A chaotic Farey tale". In: *Physical Review D* 55.12, pp. 7489–7510. ISSN: 1089-4918. DOI: [10.1103/physrevd.55.7489](https://doi.org/10.1103/physrevd.55.7489). URL: <http://dx.doi.org/10.1103/PhysRevD.55.7489>.
- Hobill, David, Adrian Burd, and Alan Coley (1994). *Deterministic chaos in general relativity: Proceedings of a NATO advanced research workshop on deterministic chaos in general relativity, held July 25-30, 1993, in Kananaskis, Alberta, Canada*. Plenum Press.
- Latifi, A., M. Musette, and R. Conte (1994). *The Bianchi IX (MIXMASTER) Cosmological Model is Not Integrable*. arXiv: gr-qc/9409025 [gr-qc].
- Misner, Charles W. (May 1969). "Mixmaster Universe". In: *Phys. Rev. Lett.* 22 (20), pp. 1071–1074. DOI: [10.1103/PhysRevLett.22.1071](https://doi.org/10.1103/PhysRevLett.22.1071). URL: <https://link.aps.org/doi/10.1103/PhysRevLett.22.1071>.
- Motter, Adilson E. (Dec. 2003). "Relativistic Chaos is Coordinate Invariant". In: *Physical Review Letters* 91.23. ISSN: 1079-7114. DOI: [10.1103/physrevlett.91.231101](https://doi.org/10.1103/physrevlett.91.231101). URL: <http://dx.doi.org/10.1103/PhysRevLett.91.231101>.
- Ott, Edward (2002). *Chaos in dynamical systems*. 2nd ed. Cambridge University Press.
- Strogatz, Steven (2024). *Nonlinear Dynamics and Chaos: With applications to physics, biology, chemistry, and engineering*. 3rd ed. CRC Press.
- Szydłowski, Marek (1993). "Toward an invariant measure of chaotic behaviour in general relativity". In: *Physics Letters A* 176.1, pp. 22–32. ISSN: 0375-9601. DOI: [https://doi.org/10.1016/0375-9601\(93\)90311-M](https://doi.org/10.1016/0375-9601(93)90311-M). URL: <https://www.sciencedirect.com/science/article/pii/037596019390311M>.

LAHORE UNIVERSITY OF MANAGEMENT SCIENCES

ON CHAOS IN GENERAL RELATIVITY

MUHAMMAD HASHIR HASSAN KHAN

Student No. 24100111

LAHORE, MAY 2024